

## Chain and Ion Dynamics in Precise Polyethylene Ionomers

Amalie L. Frischknecht,<sup>\*,†,‡</sup> Benjamin A. Paren,<sup>‡,§</sup> L. Robert Middleton,<sup>‡</sup> Jason P. Koski,<sup>†,§</sup> Jacob D. Tarver,<sup>§</sup> Madhusudan Tyagi,<sup>§,⊥</sup> Christopher L. Soles,<sup>§</sup> and Karen I. Winey<sup>\*,‡,§</sup>

<sup>†</sup>Center for Integrated Nanotechnologies, Sandia National Laboratories, Albuquerque, New Mexico 87185, United States

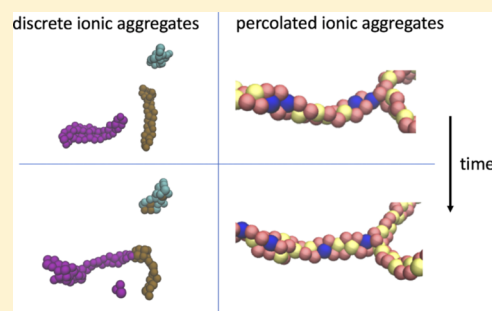
<sup>‡</sup>Department of Materials Science and Engineering and Department of Chemical and Biomolecular Engineering, University of Pennsylvania, Philadelphia, Pennsylvania 19104, United States

<sup>§</sup>NIST Center for Neutron Research, Gaithersburg, Maryland 20899-1070, United States

<sup>⊥</sup>Department of Materials Science and Engineering, University of Maryland, College Park, Maryland 20742, United States

### **S** Supporting Information

**ABSTRACT:** We analyze the dynamics from microsecond-long, atomistic molecular dynamics (MD) simulations of a series of precise poly(ethylene-co-acrylic acid) ionomers neutralized with lithium, with three different spacer lengths between acid groups on the ionomers and at two temperatures. At short times, the intermediate structure factor calculated from the MD simulations is in reasonable agreement with quasi-elastic neutron scattering data for partially neutralized ionomers. For ionomers that are 100% neutralized with lithium, the simulations reveal three dynamic processes in the chain dynamics. The fast process corresponds to hydration librations, the medium-time process corresponds to local conformational motions of the portions of the chains between ionic aggregates, and the long-time process corresponds to relaxation of the ionic aggregates. At 600 K, the dynamics are sufficiently fast to observe the early stages of lithium-ion motion and ionic aggregate rearrangements. In the partially neutralized ionomers with isolated ionic aggregates, the Li-ion-containing aggregates rearrange by a process of merging and breaking up, similar to what has been observed in coarse-grained (CG) simulations. In the 100% neutralized ionomers that contain percolated ionic aggregates, the chains remain pinned by the percolated aggregate at long times, but the lithium ions are able to move along the percolated aggregate. Here, the ion dynamics are also qualitatively similar to those seen in previous CG simulations.



### ■ INTRODUCTION

An understanding of dynamics in single-ion conducting polymers, such as ionomers with ionic groups covalently bonded to the polymer backbone, is needed to design these polymers for use as electrolytes. Often in ionomers, the dynamics of the ions and the polymer chains are coupled, with the ions following the slow segmental dynamics of the polymer.<sup>1–3</sup> In melt ionomers, the ions tend to self-assemble into nanoscale ionic aggregates, and the morphology of these aggregates affects both the ion and chain dynamics. In particular, isolated ionic aggregates serve as physical cross-links and can dramatically slow down segmental and chain-scale dynamics. In hydrated ionomers such as Nafion and related proton-conducting membranes, percolation of the hydrated ionic domains is needed to obtain good proton mobility and hence high conductivity.<sup>4</sup> An open question is whether high ionic conductivity can similarly be obtained in melt ionomers through percolated ionic aggregates. Early experimental investigations of dynamics in ionomer melts used rheology and dielectric spectroscopy to elucidate relaxation processes and time scales of chain and ion dynamics.<sup>5–8</sup> However, it is difficult to fully understand the dynamics unless the ionic aggregate morphology is also known.

The ionic aggregate morphology in melt ionomers can be probed experimentally by X-ray scattering and by scanning transmission electron microscopy (STEM). X-ray scattering from disordered ionic aggregates primarily shows a single broad peak at low wavevector, known as the ionomer peak.<sup>9,10</sup> In general, there is not sufficient information in the peak to determine the details of the morphology.<sup>11</sup> Determination of morphology from STEM is complicated by projection issues and has only been accomplished in a few cases.<sup>12–15</sup> An alternative is to use molecular dynamics (MD) simulations to determine the ionic aggregate morphology. MD simulations can also be used to study both the chain and ion dynamics in the melt state.

MD simulations of ionic aggregate morphology and dynamics have been carried out on a few different melt ionomers. Maranas and co-workers studied a poly(ethylene oxide) (PEO)-based ionomer using both atomistic and coarse-grained (CG) MD simulations.<sup>16–19</sup> These ionomers contained sulfonate groups placed on every 13 PEO monomers

**Received:** August 14, 2019

**Revised:** September 26, 2019

**Published:** October 11, 2019

along the polymer backbone and were 100% neutralized with Na ions. Their atomistic simulations were validated by comparison with X-ray scattering and by comparison of chain dynamics with quasi-elastic neutron scattering (QENS) data.<sup>20</sup> The atomistic MD simulations were found to contain a variety of ionic aggregates, with a significant fraction of long, extended sulfonate-Na aggregates, although no aggregates were found to percolate through the system. It was found that the larger stringy ionic aggregates facilitated charge transport along the ionic aggregates.<sup>16</sup> Subsequent simulations showed the possibility of obtaining superionic transport of charge along these ionic aggregates.<sup>17</sup> A CG model of the same system was derived systematically from the atomistic MD simulations, and the increased computational efficiency was sufficient to study the dynamics of the ion aggregates themselves.<sup>18</sup> The CG MD simulations also found that charge was transported along stringy ionic aggregates, but in this system, the ion content is insufficient to produce enough large stringy aggregates to enhance ion transport in the system.<sup>18,19</sup>

Forsyth and co-workers performed atomistic MD simulations on poly(2-acrylamido-2-methyl-1-propane sulfonic acid) ionomers, neutralized with lithium or sodium ions.<sup>21,22</sup> They also included a second, bulky cation to reduce the strong ion aggregation in the system and found experimentally that the dynamics of the Li or Na ions in these dual-cation ionomers were decoupled from the polymer glass transition and hence presumably decoupled from the polymer segmental motion.<sup>23,24</sup> The simulations suggested that an extended ionic aggregate network is crucial to obtain good ion mobility in these ionomers.

We have been studying precise poly(ethylene-*co*-acrylic acid) ionomers through experiments and simulations.<sup>11,25–27</sup> These ionomers have strictly linear polyethylene backbones, with pendant carboxylic acid groups separated by a precise number of carbon atoms along the backbones. In a set of poly(ethylene-*co*-acrylic acid) copolymers and ionomers with a range of neutralization levels and cations, we found good agreement (in the melt state) between the structure factors calculated from atomistic MD simulations and those measured by X-ray scattering.<sup>11,28,29</sup> The MD simulations revealed a range of ionic aggregate morphologies, from isolated, compact aggregates, to stringy aggregates, to disordered (nonperiodic) systems with percolated aggregates that span the simulation box. These distinct morphologies give rise to very similar ionomer peaks, making it impossible to distinguish different disordered aggregate morphologies by scattering alone.<sup>11</sup> We have also performed MD simulations on a CG model of these polymers. The CG simulations show that ion transport is faster in systems that form percolated ionic aggregates than in systems with isolated ionic aggregates.<sup>30,31</sup> It thus seems that spatially continuous, extended aggregates are advantageous for fast ion conduction.

In recent work, we extended our previous atomistic MD simulations of the lithium-neutralized ionomers to microsecond time scales.<sup>32</sup> We examined both partially and fully neutralized systems, in which either approximately 38 or 100% of the acid groups are neutralized by Li ions. As in earlier simulations,<sup>11,28,29</sup> we found different ionic aggregate morphologies depending on the spacer length between acid groups and the degree of neutralization. In all of the 100% neutralized ionomers, the ions form percolated aggregates that span the simulation box. In the partially neutralized ionomers, there are two populations of aggregates: aggregates that include lithium

ions and aggregates consisting solely of hydrogen-bonded acid groups. The lithium-containing aggregates tend to be stringy and consist of alternating lithium ions and oxygen atoms from the COO<sup>−</sup> groups, as well as a few un-neutralized acid groups that tend to congregate at the ends or sides of the aggregates. These ionic aggregate morphologies were found to evolve slowly and only reached a steady-state distribution over hundreds of nanoseconds.

Here, we analyze the chain and lithium-ion dynamics in these long simulations. We first compare the simulations to QENS data for the partially neutralized ionomers at 423 K and find good qualitative agreement. Previous work has shown good agreement between MD simulations and QENS data for the equivalent acid copolymers.<sup>26</sup> We therefore analyze the MD simulation data in the rest of the paper. We find that the simulations are not long enough to reach the diffusive regime at either 423 or 600 K, but we can nevertheless draw conclusions about the intermediate time chain dynamics. Analysis of the intermediate scattering function  $S(Q,t)$  calculated from the simulations shows that there are three relaxation processes in the chain dynamics, which can be fit by three Kohlrausch–Williams–Watts (KWW) functions. The lithium-ion dynamics are very slow at 423 K. At 600 K, the lithium ions are found to exchange places with their neighbors in the ionic aggregates. For partially neutralized ionomers, ion transport occurs through both rearrangement of lithium ions inside an aggregate and through merging and breaking up of the ionic aggregates, while for 100% neutralized ionomers, ion transport occurs by lithium ions moving within the percolated ionic aggregates.

## MATERIALS AND METHODS

**Materials.** In this paper, we focus on a set of poly(ethylene-*co*-acrylic acid) precise polymers neutralized with lithium ions. The system nomenclature is  $p_nAA-y\%Li$ , where  $p$  indicates a precise polymer,  $n$  is the carbon spacing length ( $n = 9, 15, \text{ or } 21$ ) between pendant acrylic acid (AA) groups, and  $y$  is the percent the system is neutralized with Li<sup>+</sup> ions. (In figure legends, we will occasionally omit the “AA” and refer to the systems as  $p_n-y\%Li$  for brevity.) As an example, the structure of p15AA-38%Li is shown in Figure 1. The

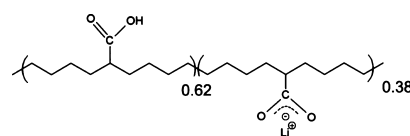


Figure 1. Structure of p15AA-38%Li.

synthesis methods of poly(ethylene-*co*-acrylic acid) precise polymers were reported previously.<sup>33–35</sup> In brief, a symmetric diene was synthesized with a protected AA group, these macromonomers were polymerized using acyclic diene metathesis, and then the double bonds were hydrogenated and the acid groups were deprotected. Neutralization with lithium proceeded as described previously.<sup>36</sup> We note that the glass-transition temperatures for the ionomers were found to be  $T_g = 342$  K for p9AA-35%Li and  $T_g = 326$  K for p15AA-38%Li. The longer spacer ionomer, p21AA-38%Li, was found to have a melting temperature of 319 K.<sup>36</sup> All experiments and simulations reported here are performed at temperatures well above  $T_g$  and  $T_m$ .

**Quasi-Elastic Neutron Scattering.** The QENS experiments were performed using a time-of-flight spectrometer, the disc chopper spectrometer (DCS), at the NIST Center for Neutron Research. Solid polymer films were melt-pressed in a Carver 4122 hot press above the  $T_g$  or  $T_m$  for 20 min. The films were then cooled to room temperature at a rate of  $\sim 15$  °C/min through a heat exchanger with circulating tap

water. The samples were prepared with a thickness of  $\sim 0.15$  mm to achieve a transmission of approximately 90% of the incident neutron beam and thereby minimize the contribution of multiple scattering; it is appropriate to assume that each neutron reaching the detectors has only scattered once. Samples were wrapped in a thin aluminum foil having the same inner circumference as the sample holder and sealed into cylindrical aluminum sample holders under helium gas in a glovebox.

Two incident neutron energies were used in the DCS, 5.665 and 13.089 meV ( $\lambda = 3.8$  and  $2.5$  Å, respectively), yielding two energy resolution settings (full width at half-maximum of the elastic peak) of  $\Delta E = 229.1$  and  $772.6$   $\mu\text{eV}$ , respectively. The elastic or instrumental resolution was collected on p9AA and cooled down to 20 K, where we assume that all of the molecular motions in the sample are frozen out and assumed to be the same for all other compositions. Background from a blank aluminum sample holder, dark counts of the detector, and a vanadium calibration standard were accounted for during data reduction. The accessible  $Q$ -ranges were  $0.144 \text{ \AA}^{-1} < Q < 3.108 \text{ \AA}^{-1}$  and  $0.219 \text{ \AA}^{-1} < Q < 4.723 \text{ \AA}^{-1}$  for the low and high incident energies, respectively. The raw data were reduced and Fourier-transformed using the Data Analysis and Visualization Environment (DAVE) software developed by NIST.<sup>37</sup>

Information on the dynamics of the sample is obtained by analyzing the change in energy of the scattered neutrons. In these samples, the incoherent scattering cross section of hydrogen is approximately an order of magnitude greater than its coherent counterpart and greater than the total cross sections of carbon and oxygen. The collected scattering is therefore dominated by incoherent scattering from the hydrogens of the PE backbone and from the single hydrogen associated with the AA. The momentum and energy-transfer dependence of the incoherent scattering  $I_{\text{exp}}(Q, \omega)$  is related via Fourier transformation to the intermediate scattering function  $S(Q, t)$ , taking into account the instrumental resolution effects through the measured instrumental resolution function  $R(Q, \omega)$

$$S(Q, t) = \frac{\int I_{\text{exp}}(Q, \omega) e^{i\omega t} d\omega}{R(Q, \omega) e^{i\omega t}} \quad (1)$$

The  $S(Q, t)$  data were normalized by  $S(Q, t = 0)$ ; however, a small vertical shift factor ( $\leq 10\%$ ) was used to match the simulation dynamics. Here, we used the same shifts as in our previous study of the acid copolymers; the QENS data were shifted vertically for p21AA-38%Li, p15AA-35%Li, and p9AA-35%Li by 0.05, 0.1, and 0.1, respectively, with the same shift factor applied for all  $Q$ . The QENS data reported here were collected at 423 K.

**MD Simulations.** Simulations were performed on ionomers neutralized either partially or fully with  $\text{Li}^+$ , at 423 and 600 K; the six systems simulated are listed in Table 1. The backbone chain lengths

**Table 1. Systems and Parameters for MD Simulations<sup>a</sup>**

system	# backbone C	# $\text{Li}^+$	$L$ (nm) at 423 K	$L$ (nm) at 600 K
p9AA-35%Li	81	269	5.98	6.15
p9AA-100%Li	81	720	5.94	6.09
p15AA-38%Li	90	182	6.15	6.40
p15AA-100%Li	90	480	6.10	6.21
p21AA-38%Li	84	117	5.98	6.33
p21AA-100%Li	84	320	5.95	6.00

<sup>a</sup> $L$  is the simulation box length.

were kept roughly constant, while preserving the precise spacing of acid groups along the chains. The partial neutralization levels were chosen to match with those of the experimental systems.

The MD simulations are the same as those described in our previous work.<sup>32</sup> We used the recent LOPLS-AA force field, which was developed by Siu et al. to improve the properties of long alkanes.<sup>38</sup> Simulations were performed using LAMMPS,<sup>39</sup> with a real-space nonbonded cutoff of 12 Å and the particle–particle–particle–

mesh solver for electrostatics. Initial states for each system were created using configurational-bias Monte Carlo simulations via the Enhanced Monte Carlo package,<sup>40,41</sup> which builds the system near the desired density. After equilibration (see the Supporting Information), simulations were run for at least 700 ns and longer than 1  $\mu\text{s}$  in many cases. All simulation boxes were cubic, with box lengths  $L$  reported in Table 1. The time-dependent radial distribution function  $G(r, t)$  for the hydrogens, that is, the self-part of the van Hove correlation function  $G_s(r, t)$ , was calculated directly from the MD simulations. The self-part of the intermediate scattering function  $S(Q, t)$  was calculated by Fourier transformation of  $G_s(r, t)$

$$S(Q, t) = \int_0^\infty G_s(r, t) r^2 \frac{\sin(Qr)}{Qr} dr \quad (2)$$

$S(Q, t)$  was normalized to  $S(Q, 0) = 1$  at high  $Q$ .

Quantities were calculated from the simulations by averaging over times for which the ionic aggregate morphologies reached an approximate steady state or did not change significantly, as determined in our recent work.<sup>32</sup> Time-dependent quantities are averaged using a moving time origin over the simulation window. The final 100 ns of each simulation are not included in plots because of noisy statistics. Total times included in the analysis range from 540 ns up to 1200 ns, depending on the system; see the Supporting Information for detailed times. The average dynamics calculated by simulations were found to be sensitive to the enhanced dynamics of chain ends in these oligomer systems, and therefore, the dynamics of the chain ends (defined as all parts of the chains on the terminal side of the end-most acid groups) were excluded from the calculations of dynamical quantities, including  $S(Q, t)$  and mean-squared displacements (MSD). Small discontinuities in the MSD curves arise from calculations performed over simulations with snapshots saved at different frequencies, which are a partial indication of the uncertainty in the MSDs. Visualizations and movies were prepared using VMD.<sup>42,43</sup>

## RESULTS

**Dynamics at 423 K.** In our previous work, we found that at 423 K, the ion aggregate distributions did not reach a steady state over the course of the simulations.<sup>32</sup> Nevertheless, the structure factors calculated from the simulations were insensitive to changes in the ionic aggregate morphologies during the simulations; the structure factors for each system showed no significant change when calculated over widely different time scales and for different ionic aggregate distributions. Furthermore, we found good agreement between the calculated structure factors and those measured by X-ray scattering. This is essentially because the scattering probes the average length scale between ionic aggregates or between pieces of a large ionic aggregate, and this length scale remains constant even as the stringy ionic aggregates merge and become larger with time.<sup>32</sup> Calculation of the hydrogen MSD starting at different times in the simulations likewise shows that the early time dynamics are not affected by changes in the ionic aggregate morphology (Figures S1 and S2). We therefore start by analyzing the dynamics at 423 K and will later consider dynamics at 600 K where the ionic aggregates do reach a steady state distribution.

At 423 K, the partially neutralized systems contain isolated ionic aggregates which are somewhat stringy. At 100% neutralization, all the aggregates are stringy, and they percolate through the simulation box for p9AA-100%Li and for p15AA-100%Li. For p21AA-100%Li, there is a large connected aggregate but also many smaller aggregates. Example simulation snapshots of isolated and stringy ionic aggregates are shown for p21AA in Figure 2.

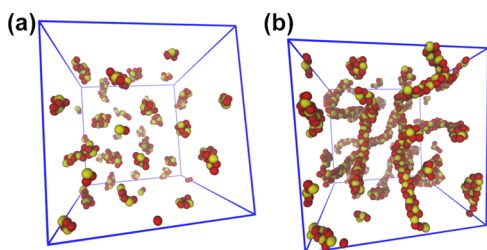


**Figure 2.** Snapshots from MD simulations at 423 K, showing only  $\text{Li}^+$  ions (yellow) and oxygen atoms (red) in  $\text{COO}^-$  groups. (a) p21AA-38%Li at  $t = 1200$  ns, which exhibits short, stringy ionic aggregates and (b) p21AA-100%Li at  $t = 940$  ns, which exhibits long, stringy ionic aggregates including some percolation. Boxes are  $L \approx 6$  nm on a side.

We first compare the intermediate structure factors calculated from the MD simulations to the QENS data at 423 K. Figure 3 shows the QENS data at selected  $Q$  values for the three partially neutralized ionomers. The intermediate scattering functions calculated from the MD simulations are

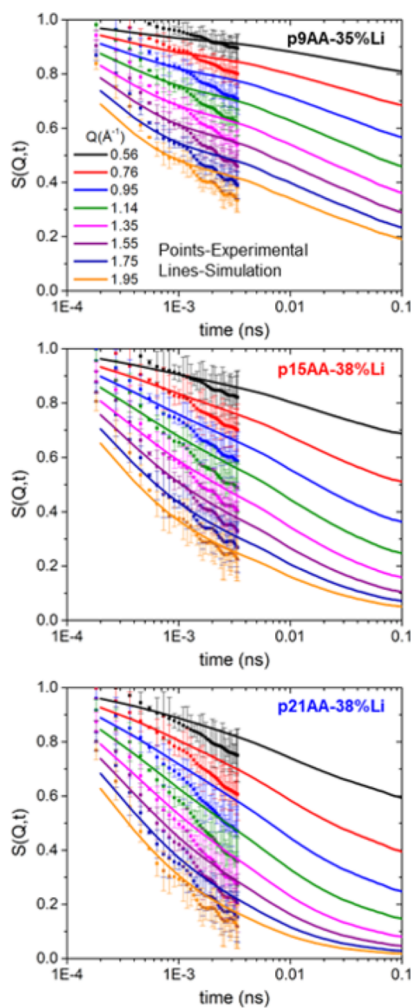


**Figure 3.** Normalized intermediate scattering function  $S(Q,t)$  calculated for neutron scattering QENS DCS data (points) and MD simulations (lines) for various  $Q$  at 423 K. The QENS data were shifted vertically for p21AA-38%Li, p15AA-38%Li, and p9AA-35%Li by 0.05, 0.1, and 0.1, respectively, for all  $Q$  values. Error bars represent one standard deviation.

shown as solid curves. The  $Q$  values range from values larger than that of the amorphous halo in the structure factor (near  $Q = 1.3 \text{ \AA}^{-1}$ ) to a low value of  $Q = 0.56 \text{ \AA}^{-1}$ , which is slightly larger than the  $Q$  of the ionomer peak, which occurs at  $Q^* = 0.494, 0.394,$  and  $0.332 \text{ \AA}^{-1}$ , for p9AA-35%Li, p15AA-38%Li, and p21AA-38%Li, respectively.<sup>32</sup> Thus, the  $S(Q,t)$  in Figure 3 includes length scales ranging from the typical interchain distance to length scales on the order of the distance between ionic aggregates. Note that at small  $Q$ , corresponding to large distances, the  $S(Q,t)$  for the three spacer lengths overlap within the error bars in Figure 3, showing that at large distances at these early times, there is no influence of spacer length. At larger  $Q$  and shorter distances, the p21AA-38%Li relaxes the fastest. These observations are corroborated by the elastic incoherent structure factor shown in Figure S3.

The MD simulations and QENS data are in good qualitative agreement, with the simulations mostly falling within the experimental error bars. However, the simulations of the partially neutralized ionomers appear to have a slower decay (smaller slope) than the QENS data. Figure S4 gives comparisons of the QENS and MD data at longer time scales, which show similar trends. We previously showed very good agreement between QENS and MD for hexadecane and for polyethylene and also good agreement between QENS and MD simulations for the equivalent acid copolymers.<sup>26</sup> Because the only difference here is the addition of the lithium ions, we speculate that inaccuracies in the lithium force field may be the cause of the differences between QENS and MD for the partially neutralized ionomers. The lithium-ion force field was optimized for lithium ions in water rather than for the low dielectric environment simulated here. We also note that many researchers lower the partial charges in nonpolarizable MD simulations of ionic systems to account for missing polarization effects; we chose not to lower the partial charges, but previous work shows that full charges can lead to slower ion dynamics than are found experimentally.<sup>16</sup> Nevertheless, the good qualitative agreement gives confidence that the simulations give a reasonable description of the hydrogen dynamics in these ionomers. We will therefore focus on analyzing the MD simulation data in the rest of the paper.

The neutralization of some or all of the acid groups with lithium ions leads to slower hydrogen dynamics, both in the QENS data and in the simulations. Figure 4 shows  $S(Q,t)$  for p21AA from the simulations for the acid copolymer (calculated previously<sup>26</sup>) and for the two ionomers neutralized with

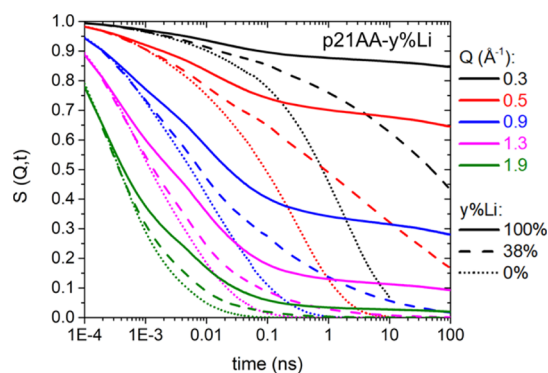


**Figure 4.**  $S(Q,t)$  calculated from the MD simulations at 423 K for p21AA (dotted curves), p21AA-38%Li (dashed curves), and p21AA-100%Li (solid curves).

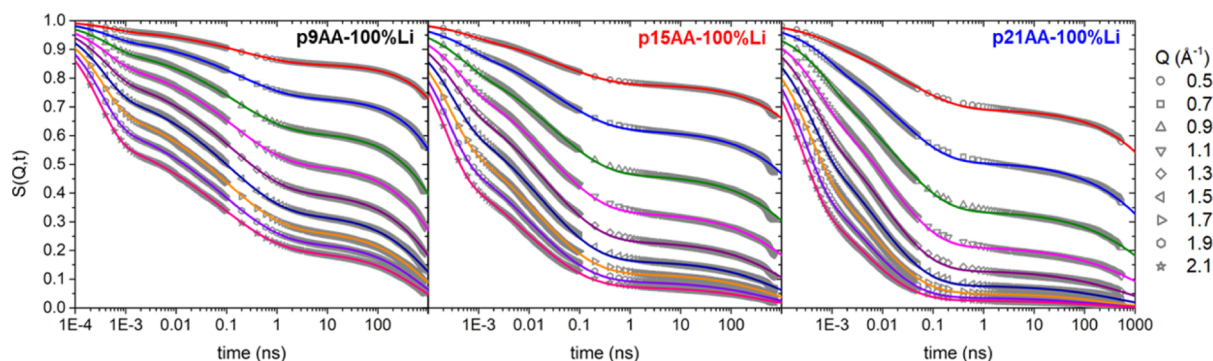


**Figure 5.**  $S(Q,t)$  calculated from the MD simulations at 423 K (points) along with fits to 3 KWW functions (curves), for p9AA-100%Li, p15AA-100%Li, and p21AA-100%Li.

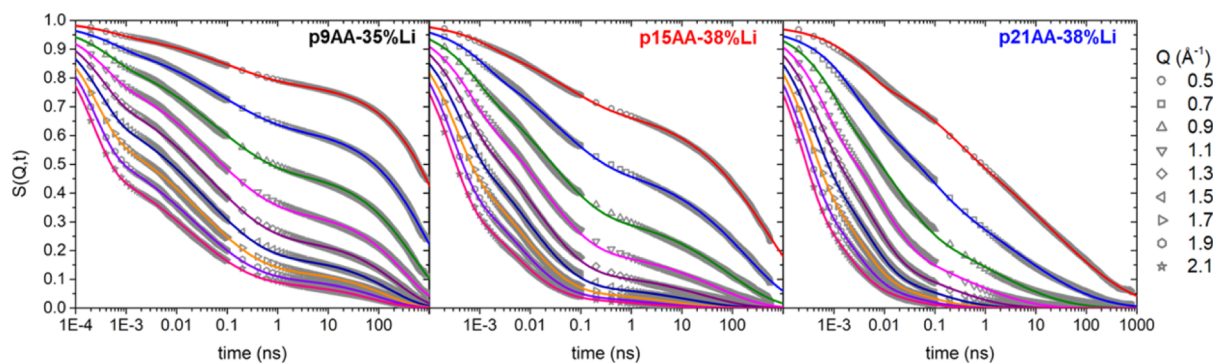


**Figure 6.**  $S(Q,t)$  calculated from the MD simulations at 423 K (points) along with fits to 3 KWW functions (curves), for p9AA-35%Li, p15AA-38%Li, and p21AA-38%Li.

lithium. For all  $Q$ , the addition of lithium ions leads to a slower decay in  $S(Q,t)$  as compared with the acid copolymer. The dynamics become increasingly slow with decreasing  $Q$ . For  $Q = 0.3 \text{ \AA}^{-1}$  near the ionomer peak ( $Q^* = 0.332 \text{ \AA}^{-1}$ ),  $S(Q,t)$  decays much more slowly with increasing concentrations of Li ions. The shapes of the  $S(Q,t)$  curves also change upon neutralization.

The full  $S(Q,t)$  MD simulation data at 423 K is shown for the 100% neutralized systems in Figure 5 and for the partially neutralized systems in Figure 6. Even at long times  $>500 \text{ ns}$ ,  $S(Q,t)$  does not decay to zero except for large  $Q$  values (small distances). Increasing ion concentrations lead to slower decay in  $S(Q,t)$  and thus slower chain dynamics; the fastest dynamics are in p21AA-38%Li and the slowest in p9AA-100%Li. As in previous studies of polymers and in our study of the acid copolymers,  $S(Q,t)$  was well-fit by two KWW functions.<sup>26</sup> In the ionomers, three KWW functions are needed to fit the simulated  $S(Q,t)$ , using

$$S(Q, t) = \phi_{\text{slow}} \exp[-(t/\tau_{\text{slow}})^{\beta_{\text{slow}}}] + \phi_{\text{med}} \exp[-(t/\tau_{\text{med}})^{\beta_{\text{med}}}] + \phi_{\text{fast}} \exp[-(t/\tau_{\text{fast}})^{\beta_{\text{fast}}}] \quad (3)$$

The solid curves through the MD data in Figures 5 and 6 show the best fits obtained using eq 3. In the partially neutralized systems, there is a coexisting population of lithium-containing aggregates and aggregates that only include acid groups. We showed previously that in the acid copolymers, the acid aggregates rearrange on time scales of roughly 1–2 ns. Clearly, the ionic aggregates rearrange much more slowly because the  $S(Q,t)$  at  $Q$  values near the ionomer peak have still

not relaxed to zero even at times approaching 1000 ns. Thus, in the partially neutralized ionomers, there is a wide distribution of relaxation time scales and very heterogeneous dynamics. By contrast, in the fully neutralized systems, all of the ionic aggregates are of similar composition, and thus, we expect these systems to have somewhat less heterogeneous dynamics. We will therefore discuss the two sets of systems separately.

The KWW fitting parameters for the three 100% neutralized ionomers are plotted as a function of  $Q$  in Figure 7. Figure 7a shows that at any given  $Q$ , increasing the ion concentration (by decreasing the spacer length) increases the slow fraction  $\phi_{\text{slow}}$  of the chain dynamics. The slow fraction is substantially larger at low  $Q$  for all three spacer lengths. Increasing ion concentration leads to a decreasing fraction of the medium-time dynamics,  $\phi_{\text{med}}$ , while the fraction of fast dynamics  $\phi_{\text{fast}}$  is relatively composition-independent. Figure 7b shows that there is a clear separation in time scales among the three KWW functions. The fastest characteristic times  $\tau_{\text{fast}}$  are insensitive to spacer length and weakly  $Q$ -dependent. The stretching parameter for the fast process  $\beta_{\text{fast}}$  was constrained to be no larger than 1 in the fits, and the fit values are  $\beta_{\text{fast}} \approx 1$  for all  $Q$  and spacer lengths, so this process is actually roughly exponential (Figure 7c). Also, values of  $\tau_{\text{fast}}$  are very similar to those found for the acid copolymers and for polyethylene in our previous work. In particular, for  $Q > 1 \text{ \AA}^{-1}$ ,  $\tau_{\text{fast}}$  has the same  $Q$  dependence and only varies by about 0.15 ps among all the acid copolymers and the 100% neutralized ionomers. We identify this fast process as corresponding to hydrogen vibrations and very local chain motions that are unrelated to any effects due to the ionic aggregates.

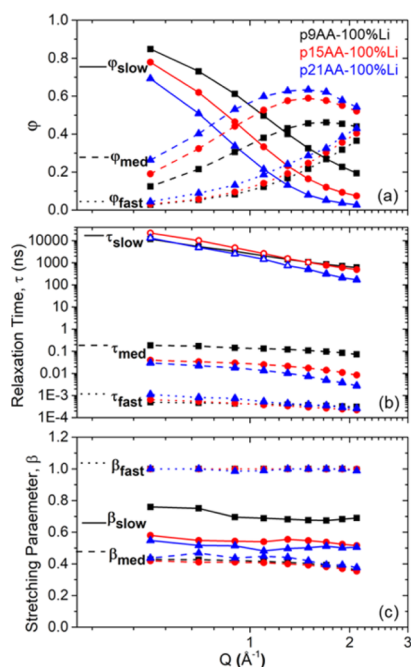


**Figure 7.** KWW fitting parameters for the fully neutralized ionomers at 423 K, showing (a) weight fractions of each KWW, (b) characteristic time scales, and (c) stretching parameters.

For both the medium and slow processes, the stretching parameters are significantly less than 1, indicating a broad range of relaxation times. The characteristic times for the medium process are longest for p9AA-100%Li and shortest for p21AA-100%Li. These times are also weakly  $Q$ -dependent. By contrast, the slow times  $\tau_{\text{slow}}$  are more strongly  $Q$ -dependent. Note that for  $Q < 1.5 \text{ \AA}^{-1}$  ( $Q < 1.3 \text{ \AA}^{-1}$  for p21AA-100%Li), the values of  $\tau_{\text{slow}}$  exceed the total simulation time. Thus, the values of  $\tau_{\text{slow}}$  must be considered as approximate.

To better understand the slow chain relaxation processes, consider the MSD of the hydrogen atoms, Figure 8. These MSDs were averaged over all hydrogen atoms in the middle portions of the chains. At very early times,  $t < 3 \times 10^{-4}$  ns, the MSDs converge for all the systems. These times correspond to the fast process, which is independent of composition. Here,

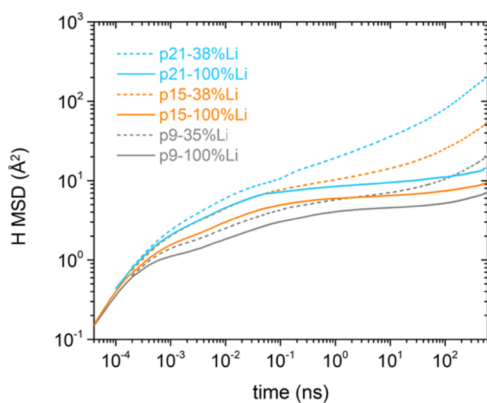


**Figure 8.** Mean-squared displacement of hydrogen atoms (neglecting chain ends) as a function of time at 423 K, for p21-38%Li (blue dashed), p21-100%Li (blue solid), p15-38%Li (orange dashed), p15-100%Li (orange solid), p9-35%Li (gray dashed), and p9-100%Li (gray solid).

the MSDs have a slope of 1, corresponding to a diffusive process. The fast characteristic times ( $\tau_{\text{fast}}$ ) correspond with those previously identified with torsional librations in long alkane chains.<sup>44,45</sup> At times longer than the longest  $\tau_{\text{fast}}$   $t > 10^{-3}$  ns, the MSDs diverge from each other, with the highest ion concentration having the smallest MSD and the lowest ion concentration having the largest MSD for any given time. Here, the ionic aggregates start to slow down the chain dynamics, but the MSDs continue to increase. The slopes of the MSD curves become smaller around the characteristic times of the medium process,  $0.002 < t < 0.2$  ns. At larger time scales, the MSD is nearly constant for the fully neutralized ionomers, indicating almost no chain motion up to 100 ns or later. The large values of  $\tau_{\text{slow}}$  extracted from  $S(Q,t)$  (Figure 7b) indicate that the ionic aggregates have not rearranged much by the end of the simulations. Given that the ionic aggregates form percolated or nearly percolated morphologies in these 100% neutralized ionomers, the chains are essentially trapped by the percolated aggregate for time scales  $> 0.2$  ns. These results lead us to conclude that the medium process consists of chain segmental motion in the regions between the  $\text{COO}^-$  groups, which are pinned in the ionic aggregates. In the partially neutralized ionomers, the hydrogen MSD continues to increase throughout the simulations, indicating less pinning of the chains at long times, because of the rearrangements of the acid-only aggregates (see below).

We previously showed in the acid copolymers that the chain dynamics are heterogeneous along the polymer chain, with the hydrogen atoms closest to the acid groups moving more slowly than hydrogens attached to backbone atoms further from the acid group.<sup>26</sup> This heterogeneous dynamics is also present in the ionomers. Figure 9a indicates our numbering scheme, where the hydrogens bonded to the backbone carbon with the pendant AA group are termed H-type #1, the hydrogens on the adjacent backbone carbons are labeled #2, and so forth with the H-type numbers increasing until the midpoint of the alkyl spacer is reached. Therefore, the hydrogens furthest from the acid group in p9AA, p15AA, and p21AA are H-types 5, 8, and 11, respectively. Figure 9b shows the hydrogen MSDs for p9AA-100%Li as a function of H-type at different times. The hydrogen on the polymer backbone nearest to the acid group is considerably slower than the others; near the middle of the chains, the hydrogen dynamics are similar. The slow chain dynamics near the acid groups persist throughout the length of the simulation, indicating that the chains are indeed pinned by the percolated ionic aggregate. The other two fully neutralized ionomers show similar trends (Figure S5), as did previous simulations on PEO-based ionomers.<sup>16</sup>

In the partially neutralized ionomers, the chains have more opportunities to change conformations because the acid-only aggregates more readily rearrange. The KWW fitting parameters for the partially neutralized ionomers (Figure S6) show similar (but less clear) trends to those for the 100% Li ionomers. The chains move considerably further than in the 100% neutralized ionomers, as shown by the hydrogen MSDs in Figure 8. The medium process time scale is less clear because it is within an order of magnitude of the time scale for acid aggregate rearrangement. The time scale for acid rearrangement can be inferred from the hydrogen MSDs as a function of H-type. In the acid copolymers, the acid groups rearranged on time scales of 1–2 ns, and the chain dynamics became homogeneous by about 2 ns.<sup>26</sup> Here, the chain dynamics are heterogeneous for longer times than for the acid

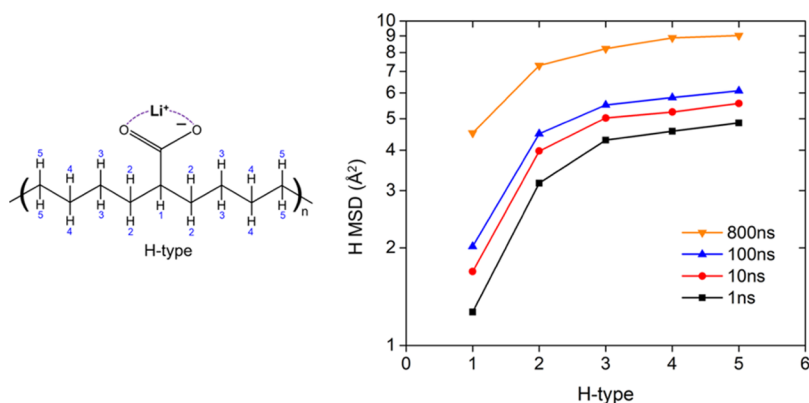


**Figure 9.** Left: Schematic showing hydrogen atoms along the polymer backbone, labeled by their distance from the acid group. Right: Mean-squared displacement of hydrogen atoms as a function of H-type at 423 K for p9AA-100%Li.

copolymers, but eventually the chain dynamics become fairly homogeneous, with all hydrogens along the polymer backbone moving a similar distance, as shown in Figure 10a for p15AA-

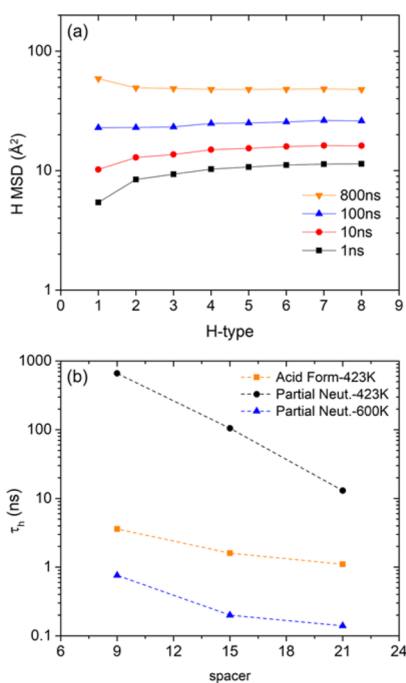


**Figure 10.** (a) Hydrogen MSDs by H-type for p15-38%Li at 423 K and various times and (b)  $\tau_h$  as a function of spacer length for the acid copolymers (orange squares), the partially neutralized ionomers at 423 K (black circles), and the partially neutralized ionomers at 600 K (blue triangles). Lines are guides to the eye.

38%Li. Note that in this case, the H-type #1 hydrogens actually have slightly larger displacements at long times than the other hydrogens; this effect is presumably due to those H-type #1 hydrogens involved in acid-only aggregates, which rearrange more quickly than aggregates containing lithium ions. To quantify when the chain dynamics become homogeneous, we calculate the time  $\tau_h$  at which the MSD for H-type #1 first becomes equal to the MSD for H-type #2, for the acid copolymers and for the partially neutralized ionomers at 423 and 600 K. As shown in Figure 10b,  $\tau_h$  for the partially neutralized ionomers at 423 K is much longer than for the acid copolymers at 423 K and is also a strong function of spacer

length, with the p21AA-38%Li ionomer showing homogenous dynamics by 13 ns, as compared with p9AA-35%Li for which  $\tau_h$  is about 660 ns. Thus, the presence of the lithium aggregates slows the chain relaxations in the partially neutralized ionomers by about 1–2 orders of magnitude compared to the acid copolymers, but the acid group rearrangements are still able to provide more chain mobility on long time scales than in the fully neutralized ionomers.

At 423 K, the lithium-ion dynamics are very slow (see Figure S7). In the fully neutralized ionomers, the lithium ions move at most 2.8 Å after 600+ ns. The largest Li-ion displacement is in the p21-38%Li ionomer, for which the Li ions have moved on average 7.2 Å after 800 ns. The average distance between Li ions in the aggregates is 2.9 Å (as determined by the Li–Li radial distribution function, see Figure S8), while the next-nearest neighbor distance is 5.5 Å (and the third-nearest distance is 8.2 Å). Thus, at 423 K, the lithium ions only move one neighbor distance in the fully neutralized ionomers, and at most two to three neighbors in the partially neutralized ionomers, during the entire course of the simulations. Because of this very slow ion dynamics, we also performed simulations at 600 K and will analyze their dynamics in the next section.

**Dynamics at 600 K.** As shown in our previous work, at 600 K, all of the 100% neutralized ionomers form percolated ionic aggregates that span the simulation box.<sup>32</sup> Figure 11 shows  $S(Q,t)$  for these fully neutralized ionomers at 600 K, along with fits to three KWW functions as defined in eq 3. We once again see very clear plateaus in  $S(Q,t)$  for times after about 0.1 ns, corresponding to slowing down of the chain dynamics because of the ionic aggregates. The KWW fit parameters are shown in Figure 12 and show similar trends to those at 423 K. Once again,  $\beta_{\text{fast}} \approx 1$  and  $\tau_{\text{fast}}$  is nearly composition- and  $Q$ -independent. Comparing the temperature dependence of the characteristic times at  $Q = 1.3 \text{ \AA}^{-1}$ , which is near the amorphous halo in the structure factor, we can see from Figure 13 that  $\tau_{\text{fast}}$  is also nearly temperature-independent. There is less separation between  $\tau_{\text{med}}$  and  $\tau_{\text{fast}}$  at 600 K than at 423 K, but the composition dependence is similar. The values of  $\tau_{\text{med}}$  are shorter at 600 K than at 423 K. This is also true for  $\tau_{\text{slow}}$ , but even at 600 K, the values of  $\tau_{\text{slow}}$  exceed the simulation time for  $Q < 1.3 \text{ \AA}^{-1}$  ( $Q < 1.1 \text{ \AA}^{-1}$  for p21AA-100%Li). Note that at high  $Q$ , the slow dynamics are a fairly small fraction of the total contribution to  $S(Q,t)$  as shown in Figure 12a.

The partially neutralized ionomers all have isolated ionic aggregates that do not percolate through the system, along

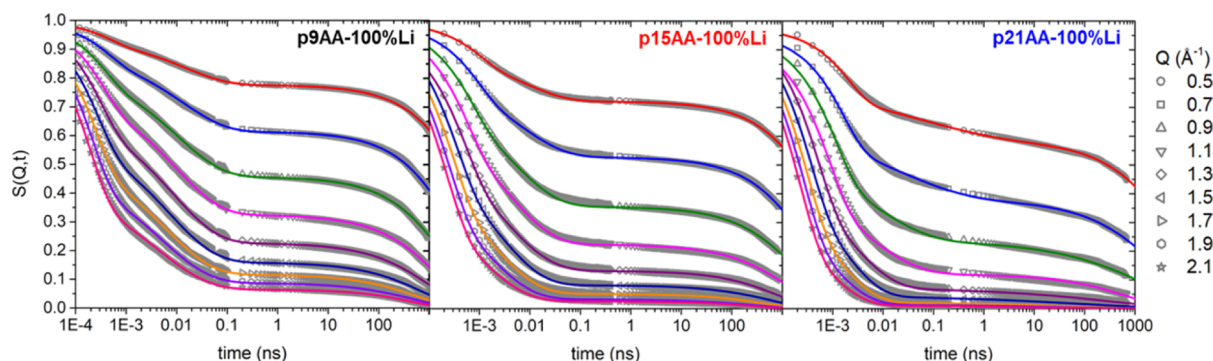


**Figure 11.**  $S(Q,t)$  calculated from the MD simulations at 600 K (points) along with fits to the three KWW functions (curves), for p9AA-100%Li, p15AA-100%Li, and p21AA-100%Li.

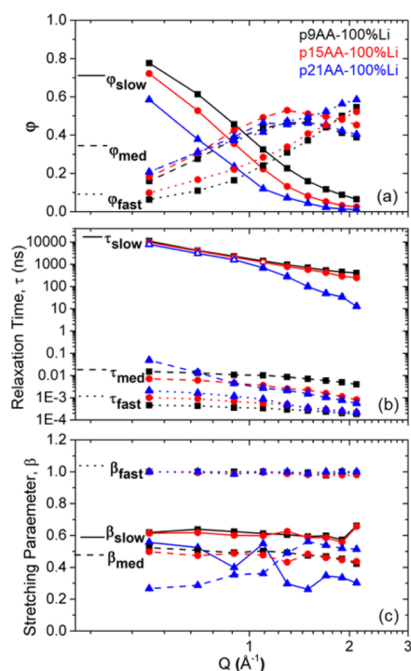


**Figure 12.** KWW fitting parameters for the fully neutralized ionomers at 600 K, showing (a) weight fractions of each KWW, (b) characteristic time scales, and (c) stretching parameters.

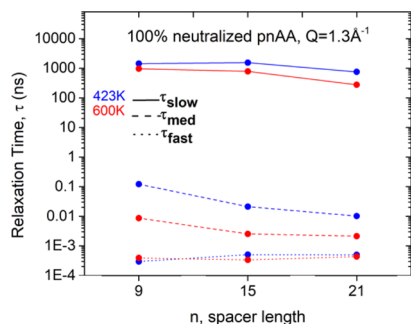


**Figure 13.** Characteristic times at  $Q = 1.3 \text{ \AA}^{-1}$  for both 423 and 600 K.

with a population of acid-only aggregates which are also isolated.<sup>32</sup> The  $S(Q,t)$  for the partially neutralized ionomers at 600 K are shown in Figure 14. At high  $Q$ ,  $S(Q,t)$  decays fairly quickly compared to the fully neutralized ionomers. This is because the polymer chains have more mobility over short distances in systems with isolated aggregates than in systems

with a percolated ionic aggregate. At lower  $Q$ , the shape of  $S(Q,t)$  is quite different from that for the fully neutralized systems. These data are not well fit by the KWW functions and we do not attempt further fitting.

Instead, we next examine the MSDs of both the hydrogen atoms and the lithium ions at 600 K. Figure 15 shows the hydrogen MSDs for all six ionomers, again only counting the hydrogens in the middle portions of the chains to avoid end effects. For the 100% neutralized ionomers, after its initial rise at early times, the MSD is nearly flat between about 0.1 ns and at least 100 ns, which falls between  $\tau_{\text{med}}$  and  $\tau_{\text{slow}}$ . The chains hardly move at all during these times because of pinning by the percolated ionic aggregates. This is confirmed by the MSDs for different hydrogen types along the backbone, which again remain heterogeneous throughout the simulations for the 100% neutralized ionomers (see Figure S9). In contrast, the chains move much more in the partially neutralized ionomers and have increasing MSDs during the simulations (Figure 15). In these systems, the acid aggregates can rearrange and facilitate the chain motion, even though the ionic aggregates have much slower dynamics. This is shown by the low values of  $\tau_{\text{h}}$  for the partially neutralized ionomers at 600 K (Figure 10b).

Figure 16 shows the MSDs for the lithium ions at 600 K. While the lithium ions move more slowly in the 100% neutralized systems than in the partially neutralized systems, the lithium ions are subdiffusive in all cases. We first discuss the partially neutralized ionomers. At late times, the MSDs for the partially neutralized ionomers have small oscillations, so we do not attempt to extract a slope. In these systems, the lithium ions move by up to 10 Å on average at late times (MSDs > 100 Å), but the lithium ions move more slowly than the chains (Figure S10) and even move more slowly than the hydrogens attached to the un-neutralized COOH groups (Figure S11). At 600 K, the dynamics are sufficiently fast to observe some ionic aggregate rearrangements in the partially neutralized ionomers, as shown in Figure 5 of ref 32. Examination of simulation trajectories shows that the ionic aggregates move diffusively together and sometimes merge with other aggregates or break up. An example is shown in Figure 17, which shows three ionic aggregates in p9AA-35%Li at different times. At the earliest time, the three aggregates (purple, brown, and cyan) are separated from each other; they are shown in the box with all the other aggregates shown in diffuse colors. By 327 ns, the brown and cyan aggregates have merged. The next event occurs around 403 ns, when the merged cluster breaks into two pieces; some of the ions that were originally in the brown

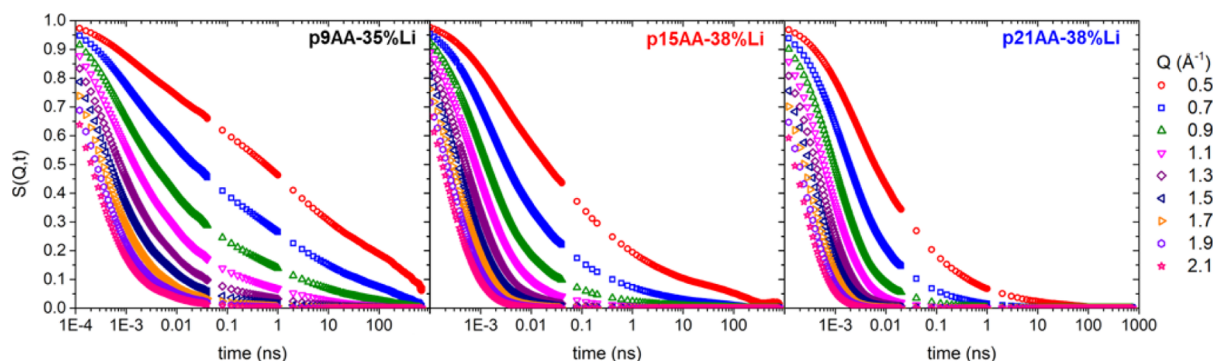


**Figure 14.**  $S(Q,t)$  calculated from the MD simulations at 600 K (points) for p9AA-35%Li, p15AA-38%Li, and p21AA-38%Li.

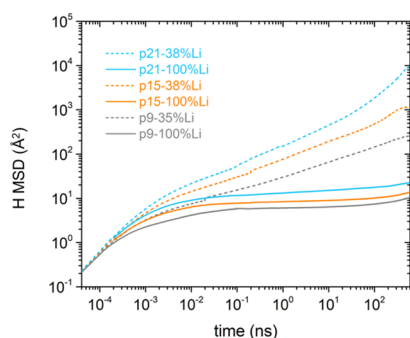


**Figure 15.** Mean-squared displacement of hydrogen atoms (neglecting chain ends) as a function of time at 600 K, for p21-38%Li (blue dashed), p21-100%Li (blue solid), p15-38%Li (orange dashed), p15-100%Li (orange solid), p9-35%Li (gray dashed), and p9-100%Li (gray solid).

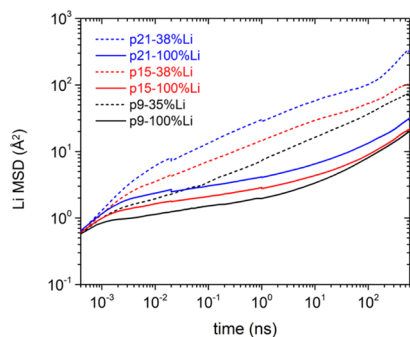


**Figure 16.** Lithium-ion MSDs at 600 K for partially neutralized (dashed curves) and fully neutralized (solid curves) ionomers.

cluster are now with the original members of the cyan cluster. Around 453 ns, the brown aggregate merges with the purple one, and one ion pair (a Li ion and two charged oxygens) separates from the purple aggregate (see [Supporting Information Movie S1](#)). This merge and break-up mechanism allows for the lithium ions to move and is qualitatively similar to the mechanism for ionic aggregate motion observed in CG simulations of ionomers when the ionic aggregate morphology consists of discrete, nonpercolated aggregates.<sup>30</sup>

For the 100% neutralized systems, the Li MSDs have slopes of about 0.5 between 600 and 800 ns. Interestingly, at long times in the 100% neutralized ionomers, the lithium ions begin to show larger average displacements than the hydrogens and the backbone carbons, as demonstrated in [Figure 18](#). While the chains are still not moving much because of the percolated ionic aggregate, the lithium ions are able to move more than

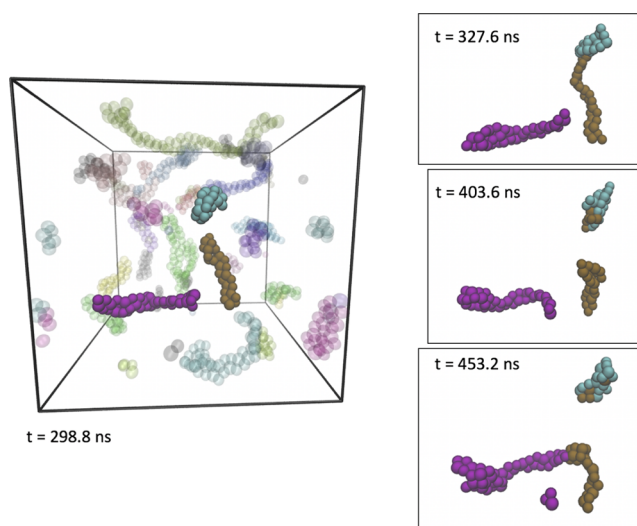


**Figure 17.** Clusters in p9AA-35%Li at 600 K and four different times. Aggregates were determined at  $t = 0$  and assigned unique colors; all ions keep the same color at later times. Only charged oxygens and Li ions are shown.

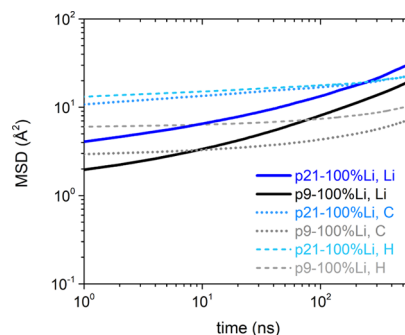


**Figure 18.** MSDs for lithium (dark blue), hydrogen (light blue dashed), and backbone carbons (light blue dotted) in p21-100%Li and MSDs for lithium (black), hydrogen (gray dashed), and backbone carbons (gray dotted) in p9-100%Li, at 600 K.

the chains themselves at these long times. This implies that the lithium ions are diffusing along the percolated aggregate. In the 100% neutralized ionomers, the lithium-ion MSD first crosses the backbone carbon MSD at  $\sim 9$  ns for p9AA-100%Li,  $\sim 46$  ns for p15AA-100%Li, and  $\sim 223$  ns for p21AA-100%Li. This is promising evidence that percolated ionic aggregates can facilitate ion conduction because they provide pathways for ion transport that are decoupled from the polymer chain

motion. The crossing of the MSD curves for the cation and for the polymer backbone atoms was also observed in our previous CG simulations of ionomers and ionenes.<sup>30</sup> An example is shown in Figure S12, using the data from ref 30.

Examination of simulation trajectories shows that the lithium ions do indeed move along the percolated ionic aggregate at long times in the 100% neutralized ionomers. This is visualized in the snapshots shown in Figure 19 for p9AA-

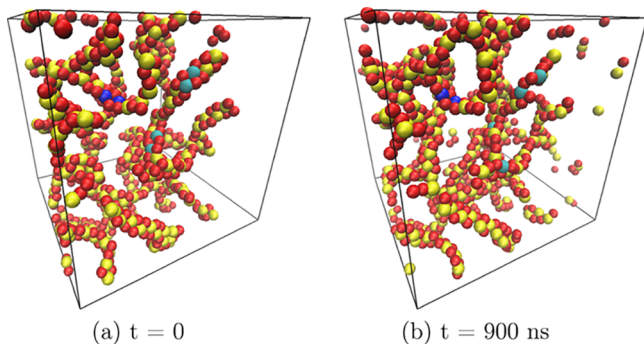


**Figure 19.** Snapshots of p9AA-100%Li at 600 K, at two times, showing oxygen (red), lithium (yellow), and three pairs of lithium ions that are neighbors at  $t = 0$  (cyan and blue).

100%Li. Here, a  $20 \times 30 \times 60.9$  Å slice of the simulation box is rendered with oxygen atoms in red and lithium ions in yellow. Three pairs of Li ions that are adjacent to each other at the beginning of the simulation have been given different colors; the two pairs in cyan separate from each other at later times, whereas the pair in dark blue remains together throughout the simulation. The ion pairs are all separated by about 3 Å at  $t = 0$ , while by  $t = 900$  ns, the purple pairs are still separated by about 3 Å, while the other two pairs are separated by 4.59 and 9.84 Å (see also Supporting Information Movie S2). The ions move by swapping places with their neighbors in the ionic aggregate, in a similar mechanism to that observed in our previous CG simulations of the ionomers.<sup>30</sup>

The similarity in ion transport mechanisms between the atomistic MD simulations and our previous CG simulations, for both isolated and percolated ionic aggregate morphologies, gives further confidence that the CG simulations captured the essential physics in these precise ionomers. This gives further support to the conclusions drawn from the CG simulations; in particular, the finding that ionic conductivity is substantially higher for systems that form percolated ionic aggregates.<sup>30,31</sup>

## CONCLUSIONS

We have studied the chain and lithium-ion dynamics in microsecond-long atomistic MD simulations of precise poly(ethylene-co-acrylic acid) ionomers. At short times, the intermediate structure factor calculated from the MD simulations is in reasonable agreement with QENS data for partially neutralized ionomers. For ionomers that are 100% neutralized with lithium, the simulations reveal three dynamic processes in the chain dynamics. The fast process corresponds to hydration librations, the medium time process corresponds to local conformational motions of the portions of the chains between ionic aggregates, and the long-time process corresponds to relaxation of the ionic aggregates. In the partially neutralized ionomers, the acid-only aggregates rearrange much more quickly than the ionic aggregates,

leading to extremely broad ranges of relaxation times and to faster decays for  $S(Q,t)$  than for the fully neutralized ionomers.

At 600 K, the dynamics are sufficiently fast to observe the early stages of lithium-ion motion and ionic aggregate rearrangements. In the partially neutralized ionomers, the acid-only aggregates rearrange relatively quickly, leading to homogeneous dynamics along the polymer backbone for times between 0.1 and 1 ns. The Li-ion containing aggregates in the partially neutralized ionomers rearrange by a process of merging and breaking up, similar to what has been observed in CG simulations. In the 100% neutralized ionomers, the chains remain pinned by the percolated aggregate at long times, while the lithium ions are able to diffuse along the percolated aggregate. Although the simulations were not long enough to reach the diffusive regime, the early time dynamics imply that ions travel along percolated ionic aggregates, and this may contribute to enhanced ionic conductivity in ionomers with percolated morphologies. In these precise polyethylene-based ionomers, the ions are too tightly associated with the  $\text{COO}^-$  groups to have good mobility and hence high conductivities, even in systems that form percolated aggregates. Practical single-ion conducting polymers would thus need to have mobile ions that more easily dissociate from the ionic groups on the polymer. Nevertheless, the mechanisms found here indicate that percolated ionic morphologies are important to efficient ion transport. This mechanism of ion transport decouples ion and polymer dynamics, which is a promising direction for polymer electrolyte design.

## ASSOCIATED CONTENT

### Supporting Information

The Supporting Information is available free of charge on the ACS Publications website at DOI: 10.1021/acs.macromol.9b01712.

Cluster dynamics in p9AA-35%Li at 600 K, at 0.8 ns per frame (MPG)

Lithium ion motion in p9AA-100%Li at 600 K, at 0.8 ns per frame (MPG)

Equilibration details for the MD simulations; additional QENS results; additional simulation results showing complete sets of data for all systems; and MSD data from previous CG simulations (PDF)

## AUTHOR INFORMATION

### Corresponding Authors

\*E-mail: alfrisc@sandia.gov (A.L.F.).

\*E-mail: winey@seas.upenn.edu (K.I.W.).

### ORCID

Amalie L. Frischknecht: 0000-0003-2112-2587

Benjamin A. Paren: 0000-0002-4361-5182

Jason P. Koski: 0000-0001-5740-8259

Karen I. Winey: 0000-0001-5856-3410

### Notes

The authors declare no competing financial interest.

## ACKNOWLEDGMENTS

K.I.W. and B.A.P. acknowledge funding from the National Science Foundation (NSF) DMR 1506726, NSF PIRE 1545884, and the Vagelos Institute for Energy Science and Technology at the University of Pennsylvania for a graduate

fellowship. This work was partially supported by the Sandia Laboratory Directed Research and Development Program (LDRD). This work was performed, in part, at the Center for Integrated Nanotechnologies, an Office of Science User Facility operated for the U.S. Department of Energy (DOE) Office of Science. Sandia National Laboratories is a multi-mission laboratory managed and operated by the National Technology and Engineering Solutions of Sandia, LLC., a wholly owned subsidiary of Honeywell International, Inc., for the U.S. DOE's National Nuclear Security Administration under contract DE-NA-0003525. The views expressed in the article do not necessarily represent the views of the U.S. DOE or the United States Government. This research was performed while J.D.T. held a National Research Council Research Associateship award at NIST. Certain commercial equipment, instruments, or materials are identified in this paper in order to specify the experimental procedure adequately. Such identification is not intended to imply recommendation or endorsement by the National Institute of Standards and Technology, nor is it intended to imply that the materials or equipment identified are necessarily the best available for the purpose.

## REFERENCES

- (1) Dou, S.; Zhang, S.; Klein, R. J.; Runt, J.; Colby, R. H. Synthesis and characterization of poly(ethylene glycol)-based single-ion conductors. *Chem. Mater.* **2006**, *18*, 4288–4295.
- (2) Fragiadakis, D.; Dou, S.; Colby, R. H.; Runt, J. Molecular mobility and Li<sup>+</sup> conduction in polyester copolymer ionomers based on poly(ethylene oxide). *J. Chem. Phys.* **2009**, *130*, 064907.
- (3) Diederichsen, K. M.; McShane, E. J.; McCloskey, B. D. Promising Routes to a High Li<sup>+</sup> Transference Number Electrolyte for Lithium Ion Batteries. *ACS Energy Lett.* **2017**, *2*, 2563–2575.
- (4) Kusoglu, A.; Weber, A. Z. New Insights into Perfluorinated Sulfonic-Acid Ionomers. *Chem. Rev.* **2017**, *117*, 987–1104.
- (5) Eisenberg, A.; Kim, J.-S. *Introduction to Ionomers*; John Wiley & Sons: New York, 1998.
- (6) Vanhoorne, P.; Register, R. A. Low-shear melt rheology of partially-neutralized ethylene-methacrylic acid ionomers. *Macromolecules* **1996**, *29*, 598–604.
- (7) Colby, R. H.; Zheng, X.; Rafailovich, M. H.; Sokolov, J.; Peiffer, D. G.; Schwarz, S. A.; Strzhemechny, Y.; Nguyen, D. Dynamics of lightly sulfonated polystyrene ionomers. *Phys. Rev. Lett.* **1998**, *81*, 3876–3879.
- (8) Fragiadakis, D.; Dou, S.; Colby, R. H.; Runt, J. Molecular mobility, ion mobility, and mobile ion concentration in poly(ethylene oxide)-based polyurethane ionomers. *Macromolecules* **2008**, *41*, 5723–5728.
- (9) Yarusso, D. J.; Cooper, S. L. Microstructure of ionomers: interpretation of small-angle x-ray scattering data. *Macromolecules* **1983**, *16*, 1871–1880.
- (10) Grady, B. P. Review and critical analysis of the morphology of random ionomers across many length scales. *Polym. Eng. Sci.* **2008**, *48*, 1029–1051.
- (11) Buitrago, C. F.; Bolinteanu, D. S.; Seitz, M. E.; Opper, K. L.; Wagener, K. B.; Stevens, M. J.; Frischknecht, A. L.; Winey, K. I. Direct Comparisons of X-ray Scattering and Atomistic Molecular Dynamics Simulations for Precise Acid Copolymers and Ionomers. *Macromolecules* **2015**, *48*, 1210–1220.
- (12) Benetatos, N. M.; Heiney, P. A.; Winey, K. I. Reconciling STEM and X-ray scattering data from a poly(styrene-ran-methacrylic acid) ionomer: Ionic aggregate size. *Macromolecules* **2006**, *39*, 5174–5176.
- (13) Benetatos, N. M.; Chan, C. D.; Winey, K. I. Quantitative morphology study of Cu-neutralized poly(styrene-ran-methacrylic acid) ionomers: STEM imaging, X-ray scattering, and real-space structural modeling. *Macromolecules* **2007**, *40*, 1081–1088.
- (14) Zhou, N. C.; Chan, C. D.; Winey, K. I. Reconciling STEM and X-ray scattering data to determine the nanoscale ionic aggregate morphology in sulfonated polystyrene ionomers. *Macromolecules* **2008**, *41*, 6134–6140.
- (15) Seitz, M. E.; Chan, C. D.; Opper, K. L.; Baughman, T. W.; Wagener, K. B.; Winey, K. I. Nanoscale Morphology in Precisely Sequenced Poly(ethylene-co-acrylic acid) Zinc Ionomers. *J. Am. Chem. Soc.* **2010**, *132*, 8165–8174.
- (16) Lin, K.-J.; Maranas, J. K. Cation Coordination and Motion in a Poly(ethylene oxide)-Based Single Ion Conductor. *Macromolecules* **2012**, *45*, 6230–6240.
- (17) Lin, K.-J.; Maranas, J. K. Superionic behavior in polyethylene-oxide-based single-ion conductors. *Phys. Rev. E: Stat., Nonlinear, Soft Matter Phys.* **2013**, *88*, 052602.
- (18) Lu, K.; Rudzinski, J. F.; Noid, W. G.; Milner, S. T.; Maranas, J. K. Scaling behavior and local structure of ion aggregates in single-ion conductors. *Soft Matter* **2014**, *10*, 978.
- (19) Lu, K.; Maranas, J. K.; Milner, S. T. Ion-mediated charge transport in ionomeric electrolytes. *Soft Matter* **2016**, *12*, 3943–3954.
- (20) Sinha, K.; Wang, W.; Winey, K. I.; Maranas, J. K. Dynamic Patterning in PEO-Based Single Ion Conductors for Li Ion Batteries. *Macromolecules* **2012**, *45*, 4354–4362.
- (21) Chen, X.; Chen, F.; Forsyth, M. Molecular dynamics study of the effect of tetraglyme plasticizer on dual-cation ionomer electrolytes. *Phys. Chem. Chem. Phys.* **2017**, *19*, 16426–16432.
- (22) Chen, X.; Forsyth, M.; Chen, F. Molecular dynamics study of ammonium based co-cation plasticizer effect on lithium ion dynamics in ionomer electrolytes. *Solid State Ionics* **2018**, *316*, 47–52.
- (23) Noor, S. A. M.; Gunzelmann, D.; Sun, J.; MacFarlane, D. R.; Forsyth, M. Ion conduction and phase morphology in sulfonate copolymer ionomers based on ionic liquid–sodium cation mixtures. *J. Mater. Chem. A* **2014**, *2*, 365–374.
- (24) Noor, S. A. M.; Sun, J.; MacFarlane, D. R.; Armand, M.; Gunzelmann, D.; Forsyth, M. Decoupled ion conduction in poly(2-acrylamido-2-methyl-1-propane-sulfonic acid) homopolymers. *J. Mater. Chem. A* **2014**, *2*, 17934–17943.
- (25) Hall, L. M.; Seitz, M. E.; Winey, K. I.; Opper, K. L.; Wagener, K. B.; Stevens, M. J.; Frischknecht, A. L. Ionic Aggregate Structure in Ionomer Melts: Effect of Molecular Architecture on Aggregates and the Ionomer Peak. *J. Am. Chem. Soc.* **2012**, *134*, 574–587.
- (26) Middleton, L. R.; Tarver, J. D.; Cordaro, J.; Tyagi, M.; Soles, C. L.; Frischknecht, A. L.; Winey, K. I. Heterogeneous Chain Dynamics and Aggregate Lifetimes in Precise Acid-Containing Polyethylenes: Experiments and Simulations. *Macromolecules* **2016**, *49*, 9176–9185.
- (27) Middleton, L. R.; Winey, K. I. Nanoscale Aggregation in Acid- and Ion-Containing Polymers. *Annu. Rev. Chem. Biomol. Eng.* **2017**, *8*, 499–523.
- (28) Bolinteanu, D. S.; Stevens, M. J.; Frischknecht, A. L. Atomistic Simulations Predict a Surprising Variety of Morphologies in Precise Ionomers. *ACS Macro Lett.* **2013**, *2*, 206–210.
- (29) Bolinteanu, D. S.; Stevens, M. J.; Frischknecht, A. L. Influence of Cation Type on Ionic Aggregates in Precise Ionomers. *Macromolecules* **2013**, *46*, 5381–5392.
- (30) Hall, L. M.; Stevens, M. J.; Frischknecht, A. L. Dynamics of Model Ionomer Melts of Various Architectures. *Macromolecules* **2012**, *45*, 8097–8108.
- (31) Ting, C. L.; Stevens, M. J.; Frischknecht, A. L. Structure and Dynamics of Coarse-Grained Ionomer Melts in an External Electric Field. *Macromolecules* **2015**, *48*, 809–818.
- (32) Frischknecht, A. L.; Winey, K. I. The evolution of acidic and ionic aggregates in ionomers during microsecond simulations. *J. Chem. Phys.* **2019**, *150*, 064901.
- (33) Baughman, T. W.; Chan, C. D.; Winey, K. I.; Wagener, K. B. Synthesis and morphology of well-defined poly(ethylene-co-acrylic acid) copolymers. *Macromolecules* **2007**, *40*, 6564–6571.
- (34) Middleton, L. R.; Szweczyk, S.; Azoulay, J.; Murtagh, D.; Rojas, G.; Wagener, K. B.; Cordaro, J.; Winey, K. I. Hierarchical Acrylic Acid Aggregate Morphologies Produce Strain-Hardening in Precise Polyethylene-Based Copolymers. *Macromolecules* **2015**, *48*, 3713–3724.

- (35) Frischknecht, A. L.; Alam, T. M.; Azoulay, J.; Bolintineanu, D. S.; Cordaro, J. G.; Hall, L. M.; Jenkins, J. E.; Lueth, C. A.; Murtagh, D.; Rempe, S. L. B.; Stevens, M. J. *Effects of Morphology on Ion Transport in Ionomers for Energy Storage*; Sandia Technical Report, 2012; SAND2012-8304.
- (36) Middleton, L. R.; Trigg, E. B.; Yan, L.; Winey, K. I. Deformation-induced morphology evolution of precise polyethylene ionomers. *Polymer* **2018**, *144*, 184–191.
- (37) Azuah, R. T.; Kneller, L. R.; Qiu, Y.; Tregenna-Piggott, P. L. W.; Brown, C. M.; Copley, J. R. D.; Dimeo, R. M. DAVE: A Comprehensive Software Suite for the Reduction, Visualization, and Analysis of Low Energy Neutron Spectroscopic Data. *J. Res. Natl. Inst. Stand. Technol.* **2009**, *114*, 341–358.
- (38) Siu, S. W. L.; Pluhackova, K.; Böckmann, R. A. Optimization of the OPLS-AA Force Field for Long Hydrocarbons. *J. Chem. Theory Comput.* **2012**, *8*, 1459–1470.
- (39) Plimpton, S. Fast parallel algorithms for short-range molecular dynamics. *J. Comp. Physiol.* **1995**, *117*, 1–19.
- (40) in 't Veld, P. J.; Rutledge, G. C. Temperature-Dependent Elasticity of a Semicrystalline Interphase Composed of Freely Rotating Chains. *Macromolecules* **2003**, *36*, 7358–7365.
- (41) Enhanced Monte Carlo Website. <http://montecarlo.sourceforge.net> (accessed on April 15, 2016).
- (42) Humphrey, W.; Dalke, A.; Schulten, K. VMD: Visual Molecular Dynamics. *J. Mol. Graphics* **1996**, *14*, 33–38.
- (43) Stone, J. An Efficient Library for Parallel Ray Tracing and Animation. M. Sc. thesis, Computer Science Department, University of Missouri-Rolla, 1998.
- (44) Smith, G. D.; Paul, W.; Yoon, D. Y.; Zirkel, A.; Hendricks, J.; Richter, D.; Schober, H. Local dynamics in a long-chain alkane melt from molecular dynamics simulations and neutron scattering experiments. *J. Chem. Phys.* **1997**, *107*, 4751–4755.
- (45) Smith, G. D.; Paul, W.; Monkenbusch, M.; Richter, D. A comparison of neutron scattering studies and computer simulations of polymer melts. *Chem. Phys.* **2000**, *261*, 61–74.

# Supporting Information for: Chain and Ion Dynamics in Precise Polyethylene Ionomers

Amalie L. Frischknecht,<sup>\*,†</sup> Benjamin A. Paren,<sup>‡</sup> L. Robert Middleton,<sup>‡</sup> Jason P. Koski,<sup>†</sup> Jacob D. Tarver,<sup>¶</sup> Madhusudan Tyagi,<sup>¶</sup> Christopher L. Soles,<sup>¶</sup> and Karen I. Winey<sup>\*,‡</sup>

<sup>†</sup>*Center for Integrated Nanotechnologies, Sandia National Laboratories, Albuquerque, New Mexico 87185, United States*

<sup>‡</sup>*Department of Materials Science and Engineering and Department of Chemical and Biomolecular Engineering, University of Pennsylvania, Philadelphia, Pennsylvania 19104, United States*

<sup>¶</sup>*NIST Center for Neutron Research, Gaithersburg, Maryland 20899-1070, United States*

E-mail: alfrisc@sandia.gov; winey@seas.upenn.edu

## S.1 Equilibration details for MD simulations

A Nosé-Hoover thermostat with a 100.0 fs damping parameter was used to maintain the temperature at either 423 K or 600 K. The integration time step was 1.0 fs in all cases. Simulations were run in the NPT ensemble at 423 K and 1 atm for 2 ns, followed by at least 10 ns in the NVT ensemble, after which trajectories were analyzed. After approximately 100 ns at 423 K, the temperature was ramped up to 600 K for each system. Systems were further equilibrated at 600 K in the NPT ensemble for 5 ns to equilibrate the density. Further equilibration then took place in the NVT ensemble for at least 15 ns, after which trajectories were analyzed.

## S.2 Effects of averaging times

As described in the Methods section and in our previous work, the ionic aggregate morphology changed during the simulations. Unless otherwise specified, all simulation results are calculated for times after which the ionic aggregates reached an approximately steady state distribution. These times are specified in Table S1, where time  $t = 0$  is defined as the time we started analyzing simulation trajectories; in all case this was after at least 15 ns of equilibration. In the figures in the main text, averages included the full times listed in Table S1 but we do not plot the final 100 ns of simulation data due to noisy statistics.

Table S1: Averaging Times

system	late times, 600K	late times, 423 K
p9AA-35%Li	600–1300 ns	100–1100 ns
p9AA-100% Li	400–1300 ns	100–1060 ns
p15AA-38%Li	400–1300 ns	100–760 ns
p15AA-100%Li	400–1360 ns	300–1140 ns
p21AA-38%Li	500–1360 ns	300–1200 ns
p21AA-100%Li	500–1380 ns	300–940 ns

The dynamics of the chains at short times, especially on the QENS time scale, are not affected by the ionic aggregate morphology. In Figure S1 we show the mean-squared displacement for the hydrogen atoms in p21-38%Li at 423 K, calculated with time origins at either 25 ns or 620 ns into the simulations; we see the MSDs are identical for times up to  $t = 0.1$  ns. Similarly, Figure S2 shows hydrogen MSDs for three of the ionomers at 600 K, also with varying time origins. Again the dynamics are identical for times up to  $t = 0.1$  ns.

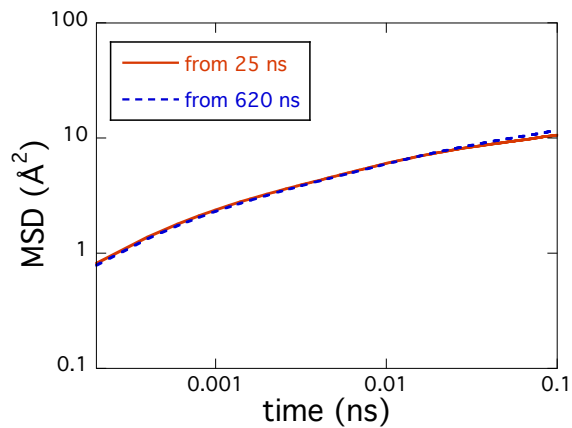


Figure S1: Comparison of hydrogen MSDs for p21-38%Li at 423K, with the time origin starting at 25 ns and 620 ns into the simulation.

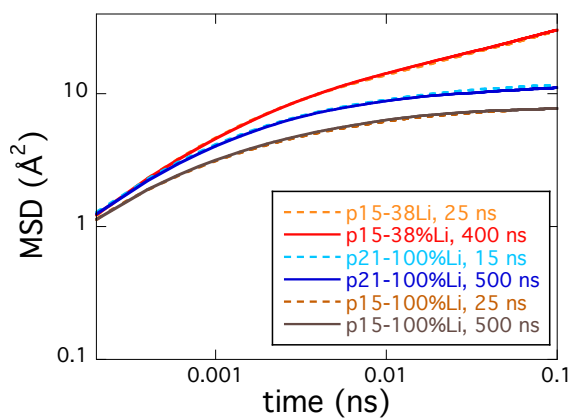


Figure S2: Comparison of hydrogen MSDs at 600 K for p15-38%Li starting at times 25 ns and 400 ns, for p21-100%Li starting at times 15 ns and 500 ns, and for p15-100%Li starting at times 25 ns and 500 ns.

### S.3 Additional QENS results

The QENS data from the disc-chopper spectrometer (DCS) were fit in the energy domain,  $S(Q, \omega)$ , using the Dave software developed by NIST. Three Lorentzian functions, that are convoluted with the resolution function, were needed to fit the data. The elastic incoherent structure factor (EISF) was calculated from the sum of all 3 Lorentzians as the inelastic pieces, and is shown at 423 K in Figure S3. The EISF represents how “elastic” or “stuck” the polymer chains are as a function of  $Q$ . Note that below the ionomer peak (low  $Q$ ) all the curves look equally stuck, due to pinning of the chains by the ionic aggregates. However, above the ionomer peak (higher  $Q$ ), chain segments are more mobile and now there is an effect of spacer length. The shorter AA segments (p9) are more stuck than the longer ones (p21). Thus spacer length affects dynamics at length scales shorter than the distance between aggregates, but not at longer length scales, in the time frame of the DCS measurements.

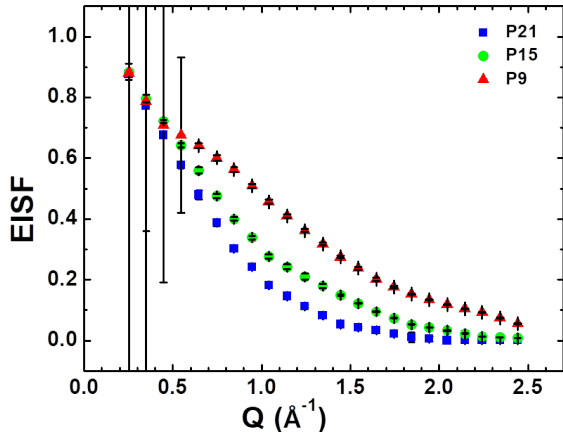


Figure S3: Elastic incoherent structure factor (EISF) from the DCS QENS measurements at 423 K, for the p21AA-38%Li (blue squares), p15AA-38%Li (green circles) and p9AA-35%Li (red triangles).

The  $S(Q, t)$  data from QENS was also calculated from the high-flux backscattering spectrometer (HFBS) and captures the longer timescales of the  $S(Q, t)$  decay to 0. QENS experiments were performed on the HFBS at the NIST Center for Neutron Research. Sample preparation was identical to the QENS DCS procedure. The incident neutron energy used was  $0.8 \mu\text{eV}$  ( $\lambda = 6.1 \text{ \AA}$ ), yielding an energy resolution (full width at half-maximum of the

elastic peak) of  $\Delta E = 61.1 \mu\text{eV}$ . The accessible  $Q$ -range was  $0.09 \text{ \AA}^{-1} < Q < 1.936 \text{ \AA}^{-1}$ . The raw data were reduced and Fourier transformed using the Data Analysis and Visualization Environment (DAVE) software developed by NIST with the same procedure specified in the manuscript.

The HFBS data is compared to the MD results in Figure S4. The experimental data were shifted down by 0.2; the absolute values of  $S(Q, t)$  for the experiments are not known and were initially normalized to  $S(Q, t^*) = 1$  where  $t^*$  is an early time on the HFBS time scale. Since some relaxation clearly occurs before this (e.g., as shown in the earlier time DCS data), the absolute values for  $S(Q, t)$  are not known. The data is somewhat noisy and Fourier transforms from the energy to the time domain can be somewhat unreliable due to boundary conditions, but again the QENS data is in qualitative agreement with the MD simulations. In particular, the data indicate that the slow relaxations found in the simulations are of similar order as the QENS data. The QENS HFBS data indicates a somewhat faster decay than the simulations, as was also seen in the comparison with the DCS data in Figure 3.

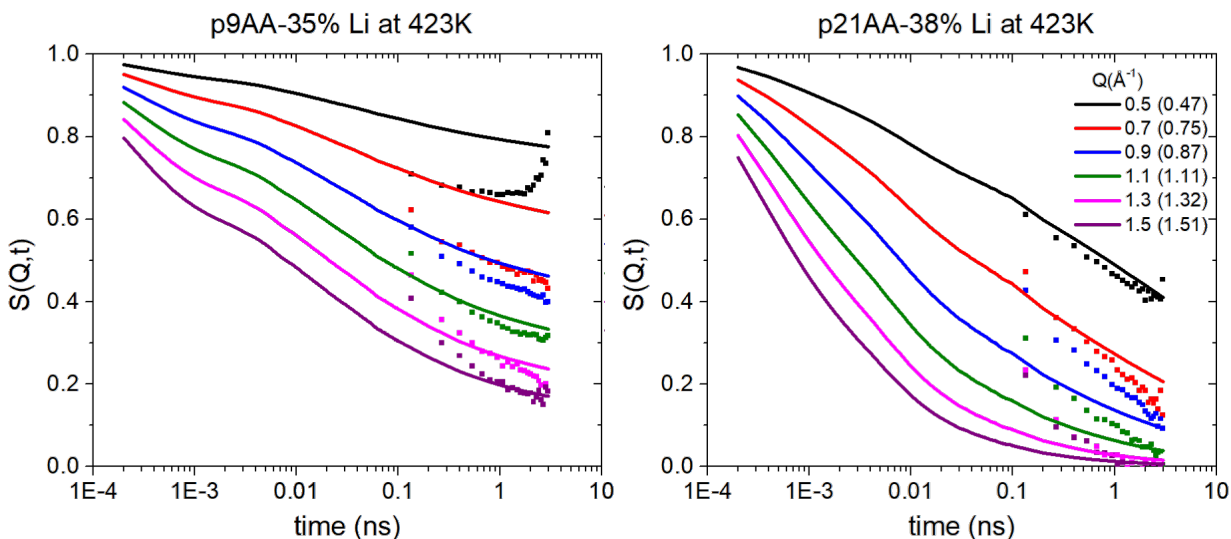


Figure S4:  $S(Q, t)$  for p9AA-35%Li (left) and p21AA-35%Li (right) from the QENS HFBS data (points) and MD simulations (curves).

## S.4 Additional simulation results

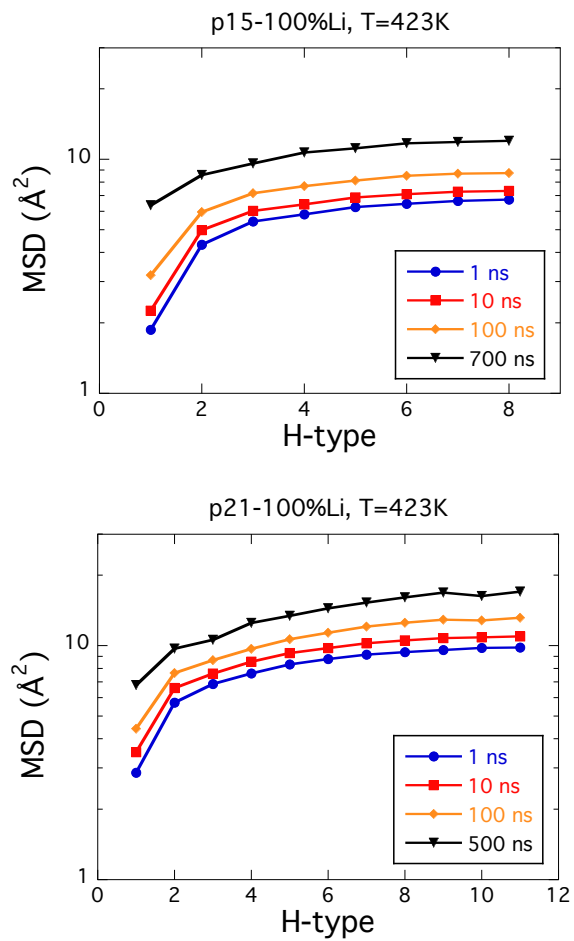


Figure S5: Hydrogen MSDs by H-type at 423 K.

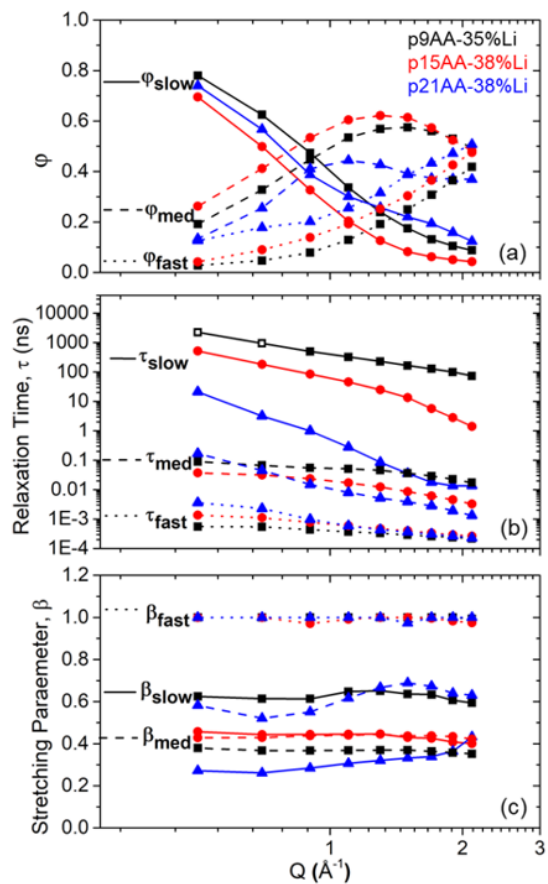


Figure S6: KWW fitting parameters for the partially neutralized ionomers at 423 K.

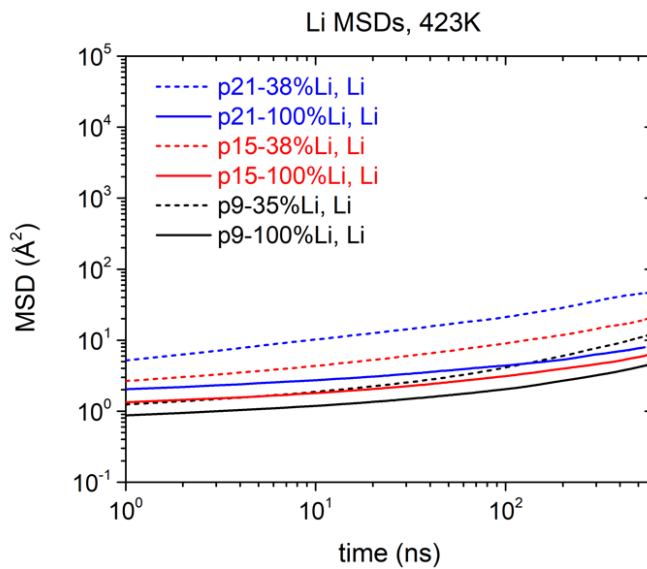


Figure S7: Lithium ion MSD at 423 K.

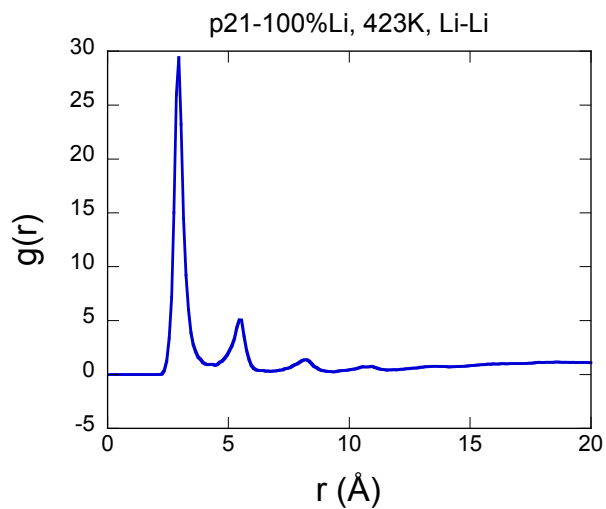


Figure S8: Lithium-lithium radial distribution function for p21AA-100%Li at 423 K. Other systems have very similar Li-Li  $g(r)$ s, with peaks in the same locations.

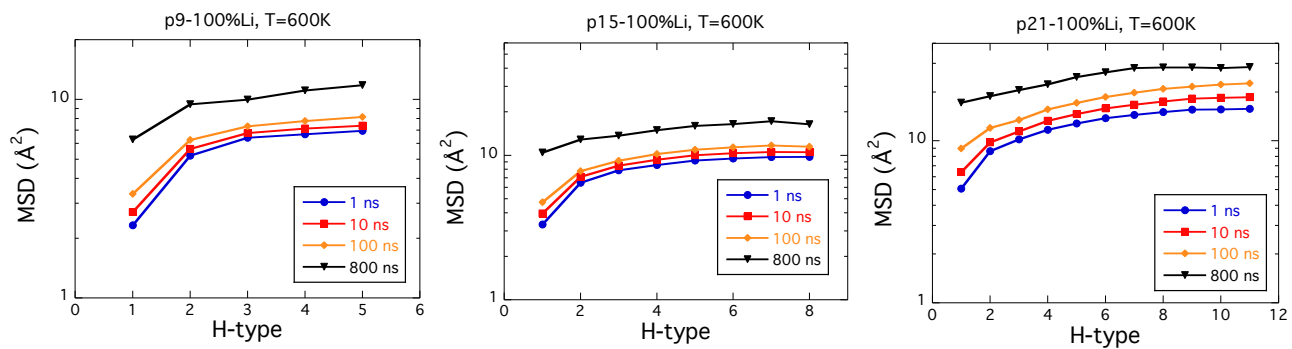


Figure S9: Hydrogen MSDs as a function of H-type at 600 K.

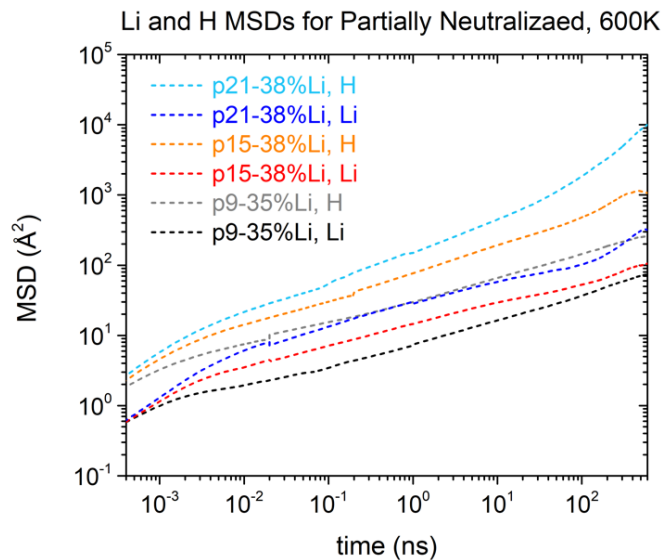


Figure S10: Comparison of hydrogen and lithium MSDs for partially neutralized ionomers at 600 K.

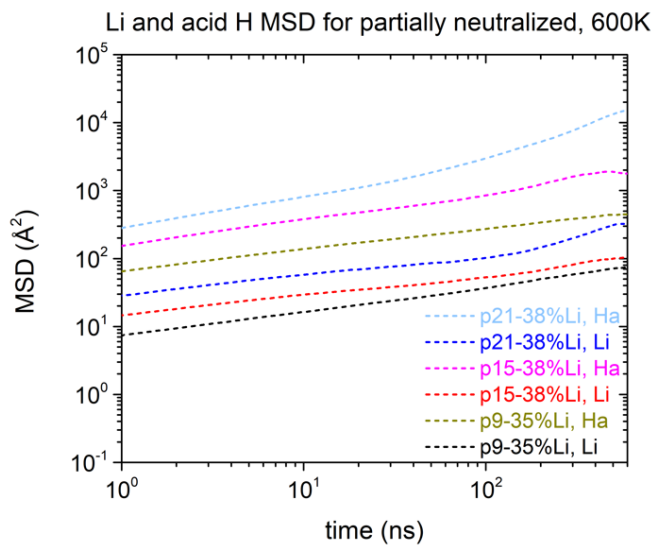


Figure S11: Comparison of acid hydrogen (Ha) and lithium MSDs for partially neutralized ionomers at 600 K. Over the simulations, the acid hydrogens move farther than the lithium ions.

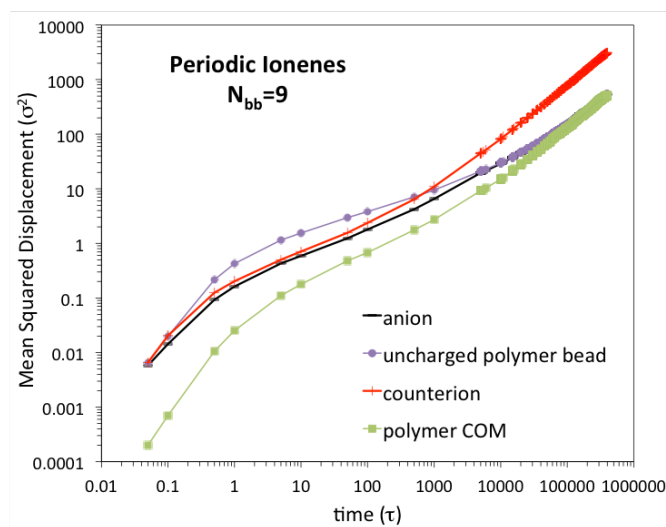


Figure S12: MSDs from coarse-grained simulations of ionenes, with charged groups placed every 9 backbone beads along the polymer. These simulations are for fully neutralized systems, and the ions form a percolated aggregate. The MSD for the cation (red) crosses that for the uncharged polymer monomers (beads, purple) at intermediate times, before becoming fully diffusive at late times. Data is from Ref 30.